

See discussions, stats, and author profiles for this publication at: <https://www.researchgate.net/publication/274643208>

# Mechanism of Rhodium-Catalyzed Cyclopropanation/Cyclization of Allenynes

ARTICLE *in* ORGANIC LETTERS · APRIL 2015

Impact Factor: 6.36 · DOI: 10.1021/acs.orglett.5b00753 · Source: PubMed

---

CITATION

1

---

READS

25

1 AUTHOR:



Genping Huang

Tianjin University

22 PUBLICATIONS 206 CITATIONS

SEE PROFILE

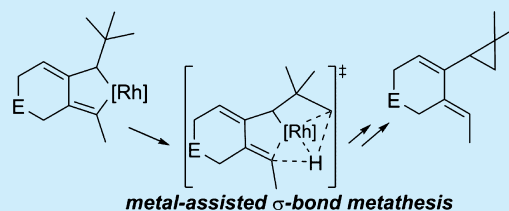
## Mechanism of Rhodium-Catalyzed Cyclopropanation/Cyclization of Allenynes

Genping Huang\*

Department of Chemistry, School of Science, Tianjin University, Tianjin 300072, P. R. China

## Supporting Information

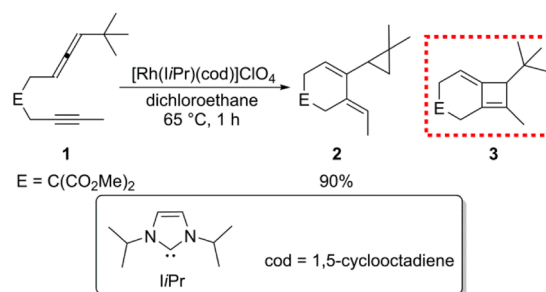
**ABSTRACT:** The rhodium-catalyzed cyclopropanation/cyclization of allenynes was investigated by means of DFT calculations. The results show that the cyclopropanation via the proposed stepwise  $C(sp^3)$ –H activation ( $\sigma$ -bond metathesis/ $C$ –H reductive elimination) was kinetically unfavorable. Instead, a concerted  $C(sp^3)$ –H activation pathway, namely the metal-assisted  $\sigma$ -bond metathesis, in which the hydrogen was directly transferred to the rhodacyclopentane assisted by the Rh center followed by a  $C$ – $C$  reductive elimination, was found to explain the experimental results.



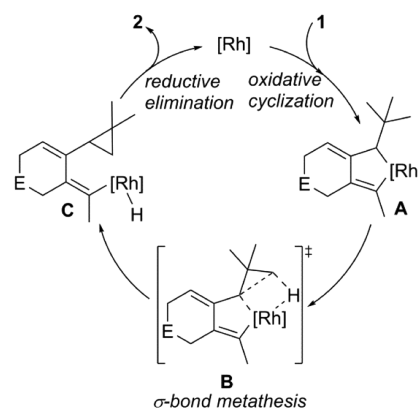
Transition-metal-catalyzed cycloaddition reactions provide one of the most powerful protocols for the construction of carbo- and heterocycles in organic synthesis.<sup>1</sup> In this context, the rhodium-catalyzed cycloadditions of enynes, diynes, dienes, and allenynes have attracted tremendous interest during the past two decades.<sup>2–4</sup> Generally, the metallacycles generated from an initial oxidative cyclization are proposed as key intermediates in these reactions. The typical reactivity of the metallacycles is that the reductive elimination could give the  $[m + n]$  cycloaddition products.<sup>3</sup> Besides, with the additional incoming unsaturated compounds, such as alkyne, alkenes, and CO, the migration insertion could occur and consequently provide an extraordinary diversity of reactions, leading to the formation of the  $[m + n + \dots + z]$  cycloaddition products.<sup>4</sup>

Recently, Oonishi, Sato, and co-workers reported a novel rhodium-catalyzed cyclopropanation/cyclization of allenynes.<sup>5</sup> The most interesting feature of this reaction is that instead of undergoing the  $[2 + 2]$  cycloaddition reaction,<sup>6</sup> it evolves through an unexpected  $C(sp^3)$ –H activation to give the cyclic product **2** exclusively (Scheme 1). Based on the experimental results,<sup>5</sup> it was proposed that (Scheme 2), after the formation of the rhodacycle intermediate **A** by an initial oxidative cyclization, the  $C(sp^3)$ –H bond of the *t*Bu group is triggered by the rhodacycle via a  $\sigma$ -bond metathesis transition state **B**, which would then generate the intermediate **C**. This intermediate **C** would undergo reductive elimination leading to the final product **2**. Later on, Mukai and co-workers in a subsequent report on the rhodium-catalyzed cycloaddition of allenylcyclopentane-alkynes further demonstrated the similar reactivity of the rhodacycle intermediate, where they found that  $C\gamma$ –H bond activation of the cyclopentane moiety could be realized by the careful selection of the rhodium catalyst.<sup>7</sup>

Considering the significance of this reaction, especially the novel reactivity of the rhodacycle intermediate, the reaction mechanism therefore deserves a more detailed investigation. Herein, we report our mechanistic study of this reaction by employing Density Functional Theory (DFT) calculations (see the Supporting Information for the computational details). The

Scheme 1. Rh-Catalyzed Cyclopropanation/Cyclization of Allenynes **1**

Scheme 2. Proposed Reaction Mechanism



calculations show that the suggested stepwise  $C(sp^3)$ –H activation ( $\sigma$ -bond metathesis/ $C$ –H reductive elimination) is however not responsible for the experimental results. Importantly, a concerted  $C(sp^3)$ –H activation pathway, namely

Received: March 15, 2015

Published: April 7, 2015

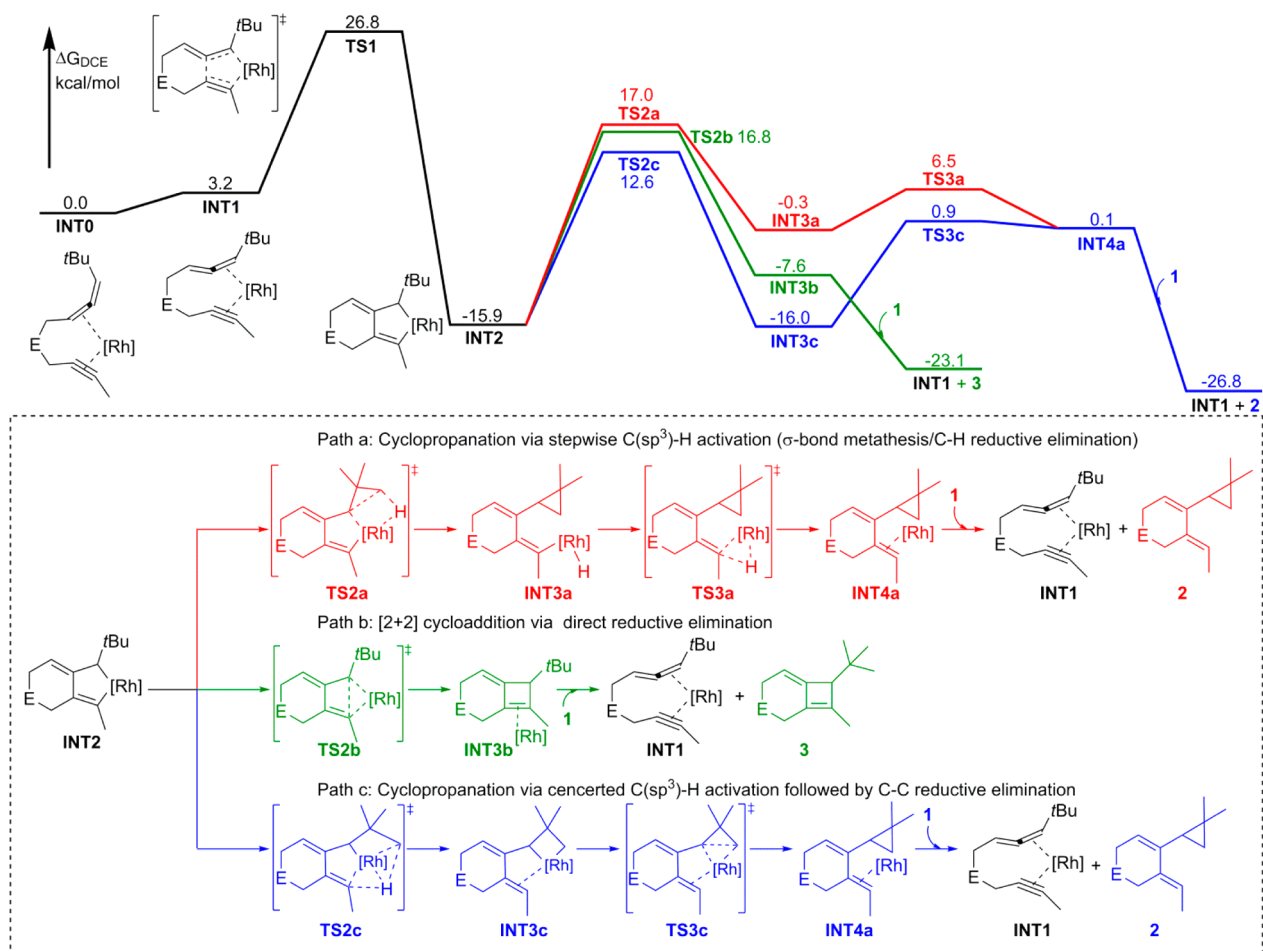


**Figure 1.** Calculated free energy profiles for the cyclopropanation/cyclization and [2 + 2] cycloaddition.

the metal-assisted  $\sigma$ -bond metathesis, followed by C–C reductive elimination, was proposed on the basis of calculations.

In experiments, the catalyst precursor is  $\text{Rh}(\text{I}i\text{Pr})\text{Cl}$  with  $\text{AgClO}_4$ , from which the neutral catalyst  $\text{Rh}(\text{I}i\text{Pr})\text{ClO}_4$  can be generated. It is possible that the active catalyst involved in the reaction is either the neutral  $\text{Rh}(\text{I}i\text{Pr})\text{ClO}_4$  catalyst or the cationic  $\text{Rh}(\text{I}i\text{Pr})^+$  catalyst. Both scenarios were thus considered and compared in our calculations, and the results show that the energies with the neutral  $\text{Rh}(\text{I}i\text{Pr})\text{ClO}_4$  catalyst are lower than those with the cationic  $\text{Rh}(\text{I}i\text{Pr})^+$  catalyst. Therefore, in the text, we will only discuss the results in the case of  $\text{Rh}(\text{I}i\text{Pr})\text{ClO}_4$ , and the results for the case of  $\text{Rh}(\text{I}i\text{Pr})^+$  are given in the Supporting Information.

The reaction begins with the coordination of **1** with  $\text{Rh}(\text{I}i\text{Pr})\text{ClO}_4$  through the allenic double bond and the alkyne moiety, which was calculated to be highly exergonic, by more than 40 kcal/mol (see the Supporting Information for details). For this step, two possible complexations can be envisioned, i.e. involving either the distal (**INT1**) or the proximal double bond (**INT0**) of the allene moiety (Figure 1). The calculations show that the **INT0** is more stable than **INT1**, by 3.2 kcal/mol (Figure 1).

According to Scheme 2, the first step of the reaction is the oxidative cyclization. The results show that, from **INT1**, the oxidative cyclization between the distal double bond of the allene and alkyne via **TS1** requires an energy barrier of 26.8 kcal/mol relative to **INT0** (Figure 1). On the other hand, although **INT0** is 3.2 kcal/mol more stable than **INT1**, the free

energy of the corresponding transition state was calculated to be higher than that of **TS1** (see the Supporting Information for details). The oxidative cyclization was found to be a highly exergonic process. The resulting intermediate is the rhodacyclopentane **INT2**, which was calculated to be 15.9 kcal/mol lower in energy than **INT0**.

Upon the formation of **INT2**, the cyclopropanation process was proposed to occur through the stepwise  $\text{C}(\text{sp}^3)$ –H activation, including  $\sigma$ -bond metathesis and C–H reductive elimination (Scheme 2 and Figure 1, Path a). The  $\sigma$ -bond metathesis was found to take place via the four-membered ring transition state **TS2a** (Figure 1). The resulting intermediate from **TS2a** is  $\text{Rh}(\text{III})$ -hydride complex **INT3a**, which was found to be 15.6 kcal/mol higher than **INT2**. From **INT3a**, the C–H reductive elimination takes place easily through the transition state **TS3a**, with an energy barrier of only 6.8 kcal/mol relative to **INT3a**, i.e. 22.4 kcal/mol relative to **INT2**. Finally, the catalytic cycle is closed by the ligand exchange step between **1** and **INT4a** to release the cyclopropanation/cyclization product **2** and regenerate the intermediate **INT1**. As shown in Figure 1, the energy barrier of cyclopropanation via the stepwise  $\text{C}(\text{sp}^3)$ –H activation is determined by the  $\sigma$ -bond metathesis step, which was calculated to be 32.9 kcal/mol relative to **INT2**.

Another possibility from **INT2**, namely the direct reductive elimination, was also calculated (Figure 1, Path b), which would give the experimentally not observed [2 + 2] cycloaddition product **3**. The corresponding transition state is **TS2b**, and the

energy barrier was calculated to be 32.7 kcal/mol relative to INT2. The resulting intermediate is INT3b, which can give the product 3 by a ligand exchange step with 1.

Therefore, the [2 + 2] cycloaddition and cyclopropanation/cyclization were calculated to have almost identical energy barriers (32.7 vs 32.9 kcal/mol), which indicates that the reaction should give both 2 and 3 with a ratio of around 50:50, being inconsistent with the experimental results that product 2 was formed exclusively. The alternative mechanism for the cyclopropanation thus must be examined to account for the experimental observations.

Indeed, during our calculations, we found that the cyclopropanation can be realized through a concerted  $C(sp^3)$ -H activation followed by C-C reductive elimination (Figure 1, Path c). As shown in Figure 1, the concerted  $C(sp^3)$ -H activation pathway was found to occur via the transition state TS2c, from which the hydrogen of the *t*Bu group was directly transferred to  $C^5$ , and simultaneously the Rh-C<sup>5</sup> was broken and Rh-C<sup>6</sup> was formed (Figure 2), resulting in the generation

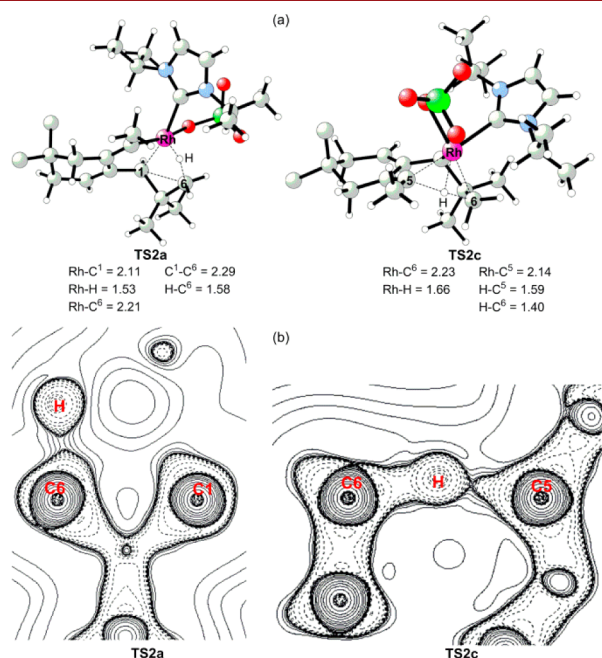


**Figure 2.** (a) Optimized structures of TS2a and TS2c, bond distances are in Å; (b) plots of the Laplacian of electron density ( $\nabla^2\rho$ ) for the transition states TS2a and TS2c in a plane defined by the two carbon atoms and hydrogen.

of the intermediate INT3c. INT3c then undergoes the C-C reductive elimination (via TS3c) to afford the intermediate INT4a, followed by a subsequent ligand exchange with 1 to produce the final product 2. The rate-determining step of this process was found to be the  $C(sp^3)$ -H activation (TS2c), with an energy barrier of 28.5 kcal/mol relative to INT2.

Compared to the cyclopropanation process via the proposed stepwise  $C(sp^3)$ -H activation, this alternative pathway was found to be more favorable by 4.4 kcal/mol (28.5 kcal/mol of Path c vs. 32.9 kcal/mol of Path a). More importantly, the energy barrier was found to be 4.2 kcal/mol lower than that of [2 + 2] cycloaddition (28.5 kcal/mol of Path c vs 32.7 kcal/mol of Path b), which corresponds to a calculated 2:3 ratio of about 518:1 (65 °C), which is in excellent agreement with the experimental outcomes that product 2 was formed exclusively.<sup>8</sup>

To the best of our knowledge, the  $C(sp^3)$ -H activation of metallacycles through type TS2c has not been previously reported, which therefore deserves particular attention. In TS2c (Figure 2), the bond distance of Rh-H is 1.66 Å, indicating that Rh-H is almost fully formed. Moreover, the breaking C<sup>6</sup>-H and the forming C<sup>5</sup>-H bonds were found to be 1.40 and 1.59 Å, respectively. Meanwhile, the breaking Rh-C<sup>5</sup> and the forming Rh-C<sup>6</sup> bonds were found to be only longer by less than 10%, compared to those in INT2 and INT3c. These geometric features indicate that TS2c is a four-center metal-assisted  $\sigma$ -bond metathesis transition state.<sup>9</sup> The reason TS2c is lower in energy than TS2a may be due to the steric repulsion in TS2a. In TS2a, the forming C<sup>1</sup>-C<sup>6</sup> is as long as 2.29 Å due to the steric repulsion between the C<sup>1</sup> and C<sup>6</sup> groups, and bond distances of C<sup>6</sup>-H, Rh-H, and Rh-C<sup>6</sup> are 1.58, 1.53, and 2.21 Å, respectively. TS2a therefore is more likely a three-center oxidatively added transition state.<sup>9a,10</sup> The Rh center in TS2a thus could be described to have Rh(V) character.<sup>11</sup> The Laplacian plots of electron density for the transition states TS2a and TS2c (Figure 2) further support that there are significant electron density concentrations between H and C<sup>5</sup> and C<sup>6</sup> in TS2c, while in TS2a, no electron density concentrations can be found between C<sup>1</sup> and C<sup>6</sup>, and moreover, the very weak electron density concentrations between C<sup>6</sup> and H indicate that the C<sup>6</sup>-H bond is almost broken.

Oonishi et al. conducted a kinetic isotope competition experiment using an equimolar mixture of allenynes 1 and [D<sub>9</sub>]-1 (the *t*Bu group of 1 is deuterium-labeled) at room temperature, and the kinetic isotope effect (KIE) was calculated to be about 3.9,<sup>5</sup> from which  $C(sp^3)$ -H activation was proposed to be the rate-determining step. To test the validity of our proposed mechanism, the KIE of the rate-determining step (INT2-TS2c) was calculated, by evaluating the zero-point energies with those of the deuterium-labeled INT2 and TS2c. The calculated zero-point energy difference is 0.73 kcal/mol, which corresponds to a calculated KIE of 3.4 at room temperature, which is in good agreement with the experimental KIE of 3.9.

In the current study, we have presented a mechanistic investigation of the rhodium-catalyzed cyclopropanation/cyclization of allenynes by means of DFT calculations. The results show that the reaction is initiated by an oxidative cyclization, resulting in the formation of the rhodacyclopentane, from which it was found that the proposed stepwise  $C(sp^3)$ -H activation through  $\sigma$ -bond metathesis/C-H reductive elimination is however kinetically unfavorable. An alternative concerted  $C(sp^3)$ -H activation mechanism, namely metal-assisted  $\sigma$ -bond metathesis, was proposed on the basis of the calculations, in which the hydrogen of the *t*Bu group was directly transferred to the rhodacyclopentane assisted by the Rh center. The catalytic cycle is finally closed by a C-C reductive elimination, leading to the final cyclopropanation/cyclization product. The metal-assisted  $\sigma$ -bond metathesis step constitutes the rate-determining step of the overall reaction.

The present calculations provide important insights into the reactivity of the rhodacycle intermediate, which should have important implications for the design of new catalytic systems. Studies on the related reaction<sup>7</sup> are currently ongoing in our laboratory.



## ■ ASSOCIATED CONTENT

### ■ Supporting Information

Computational details, additional computational results, table of calculated energies, and Cartesian coordinates of all optimized structures. This material is available free of charge via the Internet at <http://pubs.acs.org>.

## ■ AUTHOR INFORMATION

### Corresponding Author

\*E-mail: [gphuang@tju.edu.cn](mailto:gphuang@tju.edu.cn).

### Notes

The authors declare no competing financial interest.

## ■ ACKNOWLEDGMENTS

Computer time was generously provided by the ROOS cluster from Prof. Fahmi Himo's Research Group at Stockholm University, Sweden, and High Performance Computing Center of Tianjin University, P. R. China.

## ■ REFERENCES

- (1) For selected reviews, see: (a) Bruneau, C. *Angew. Chem., Int. Ed.* **2005**, *44*, 2328–2334. (b) Zhang, L.; Sun, J.; Kozmin, S. A. *Adv. Synth. Catal.* **2006**, *348*, 2271–2296. (c) Shen, H. C. *Tetrahedron* **2008**, *64*, 7847–7870. (d) Campolo, D.; Gastaldi, S.; Roussel, C.; Bertrand, M. P.; Nechab, M. *Chem. Soc. Rev.* **2013**, *42*, 8434–8466. (e) Pellissier, H.; Clavier, H. *Chem. Rev.* **2014**, *114*, 2775–2823. (f) Shibata, Y.; Tanaka, K. *Synthesis* **2012**, 323–350. (g) Broere, D. L. J.; Rujiter, E. *Synthesis* **2012**, 2639–2672. (h) Weding, N.; Hapke, M. *Chem. Soc. Rev.* **2011**, *40*, 4525–4538. (i) Pla-Quintana, A.; Roglans, A. *Molecules* **2010**, *15*, 9230–9251. (j) López, F.; Mascareñas, J. L. *Beilstein J. Org. Chem.* **2011**, *7*, 1075–1094. (k) Nakamura, I.; Yamamoto, Y. *Chem. Rev.* **2004**, *104*, 2127–2198. (l) Amatore, M.; Aubert, C. *Eur. J. Org. Chem.* **2015**, 265–286. (m) Tanaka, K.; Tajima, Y. *Eur. J. Org. Chem.* **2012**, 3715–3725. (n) Pellissier, H. *Adv. Synth. Catal.* **2011**, *353*, 189–218. (o) Jiao, L.; Yu, Z.-X. *J. Org. Chem.* **2013**, *78*, 6842–6848. (p) Inglesby, P. A.; Evans, P. A. *Chem. Soc. Rev.* **2010**, *39*, 2791–2805. (q) Croatt, M. P.; Wender, P. A. *Eur. J. Org. Chem.* **2010**, 19–32. (r) Aubert, C.; Fensterbank, L.; Garcia, P.; Malacria, M.; Simonneau, A. *Chem. Rev.* **2011**, *111*, 1954–1993. (s) Yamamoto, Y. *Chem. Rev.* **2012**, *112*, 4736–4769. (t) Aubert, C.; Buisine, O.; Malacria, M. *Chem. Rev.* **2002**, *102*, 813–834. (u) Zhang, Z.; Zhu, G.; Tong, X.; Wang, F.; Xie, X.; Wang, J.; Jiang, L. *Curr. Org. Chem.* **2006**, *18*, 1457–1478.
- (2) For selected examples, see: (a) Sugikubo, K.; Omachi, F.; Miyanaga, Y.; Inagaki, F.; Matsumoto, C.; Mukai, C. *Angew. Chem., Int. Ed.* **2013**, *52*, 11369–11372. (b) Inagaki, F.; Sugikubo, K.; Miyashita, Y.; Mukai, C. *Angew. Chem., Int. Ed.* **2010**, *49*, 2206–2210. (c) Inagaki, F.; Sugikubo, K.; Oura, Y.; Mukai, C. *Chem.—Eur. J.* **2011**, *17*, 9062–9065. (d) Wender, P. A.; Haustedt, L. O.; Lim, J.; Love, J. A.; Williams, T. J.; Yoon, J.-Y. *J. Am. Chem. Soc.* **2006**, *128*, 6302–6303. (e) Jiao, L.; Yuan, C.; Yu, Z.-X. *J. Am. Chem. Soc.* **2008**, *130*, 4421–4430. (f) Inglesby, P. A.; Bacsá, J.; Negru, D. E.; Evans, P. A. *Angew. Chem., Int. Ed.* **2014**, *53*, 3952–3956. (g) Cao, P.; Wang, B.; Zhang, X. *J. Am. Chem. Soc.* **2000**, *122*, 6490–6491. (h) Cao, P.; Zhang, X. *Angew. Chem., Int. Ed.* **2000**, *39*, 4104–4106. (i) Wender, P. A.; Williams, T. J. *Angew. Chem., Int. Ed.* **2002**, *41*, 4550–4553. (j) Sato, Y.; Oonishi, Y.; Mori, M. *Organometallics* **2002**, *22*, 30–32.
- (3) For selected examples, see: (a) Falk, A.; Fiebig, L.; Neudörfl, J.-M.; Adler, A.; Schmalz, H.-G. *Adv. Synth. Catal.* **2011**, *353*, 3357–3362. (b) Aikawa, K.; Akutagawa, S.; Mikami, K. *J. Am. Chem. Soc.* **2006**, *128*, 12648–12649. (c) Motoda, D.; Kinoshita, H.; Shinokubo, H.; Oshima, K. *Angew. Chem., Int. Ed.* **2004**, *43*, 1860–1862. (d) O'Mahony, D. J. R.; Belanger, D. B.; Livinghouse, T. *Org. Biomol. Chem.* **2003**, *1*, 2038–2040. (e) Shibata, T.; Fujiwara, D.; Endo, K. *Org. Biomol. Chem.* **2008**, *6*, 464–467. (f) Saito, A.; Ono, T.; Takahashi, A.; Taguchib, T.; Hanzawa, Y. *Tetrahedron Lett.* **2006**, *47*, 891–895. (g) Davies, D. L.; Fawcett, J.; Garratt, S. A.; Russell, D. R. *Dalton Trans.* **2004**, 3629–3634.
- (4) For selected examples, see: (a) Noucti, N. N.; Alexanian, E. J. *Angew. Chem., Int. Ed.* **2013**, *52*, 8424–8427. (b) Brummond, K. M.; Davis, M. M.; Huang, C. *J. Org. Chem.* **2009**, *74*, 8314–8320. (c) Wender, P. A.; Croatt, M. P.; Deschamps, N. M. *Angew. Chem., Int. Ed.* **2006**, *45*, 2459–2462. (d) Iwata, T.; Inagaki, F.; Mukai, C. *Angew. Chem., Int. Ed.* **2013**, *52*, 11138–11142. (e) Lainhart, B. C.; Alexanian, E. J. *Org. Lett.* **2015**, *17*, 1284–1287. (f) Evans, P. A.; Baum, E. W. *J. Am. Chem. Soc.* **2004**, *126*, 11150–11151. (g) Gilbertson, S. R.; DeBoef, B. *J. Am. Chem. Soc.* **2002**, *124*, 8784–8785.
- (5) Oonishi, Y.; Kitano, Y.; Sato, Y. *Angew. Chem., Int. Ed.* **2012**, *51*, 7305–7308.
- (6) For transition-metal-catalyzed [2 + 2] cycloaddition of allenes, see: (a) Shen, Q.; Hammond, G. B. *J. Am. Chem. Soc.* **2002**, *124*, 6534–6535. (b) Oh, C. H.; Park, D. I.; Jung, S. H.; Reddy, V. R.; Gupta, A. K.; Kim, Y. M. *Synlett* **2005**, 2092–2094. (c) Oh, C. H.; Gupta, A. K.; Park, D. I.; Kim, N. *Chem. Commun.* **2005**, 5670–5672. (d) Saito, N.; Tanaka, Y.; Sato, Y. *Org. Lett.* **2009**, *11*, 4124–4126.
- (7) Mukai, C.; Ohta, Y.; Oura, Y.; Kawaguchi, Y.; Inagaki, F. *J. Am. Chem. Soc.* **2012**, *134*, 19580–19583.
- (8) Oonishi et al. found that both cyclopropanation/cyclization and [2 + 2] cycloaddition products were observed using the IMes ligand (ref 5). Indeed, the calculated energy difference between TS2b and TS2c is only 0.1 kcal/mol for the IMes ligand, being in excellent agreement with the experimental results. See the Supporting Information for details.
- (9) (a) Vastine, B. A.; Hall, M. B. *J. Am. Chem. Soc.* **2007**, *129*, 12068–12069. (b) Hartwig, J. F.; Cook, K. S.; Hapke, M.; Incarvito, C. D.; Fan, Y.; Webster, C. E.; Hall, M. B. *J. Am. Chem. Soc.* **2005**, *127*, 2538–2552.
- (10) Lam, W. H.; Jia, G.; Lin, Z.; Lau, C. P.; Eisenstein, O. *Chem.—Eur. J.* **2003**, *9*, 2775–2782.
- (11) Wiberg bond index calculations show that the bond orders for the Rh–C<sup>1</sup>, Rh–C<sup>6</sup>, Rh–H, C<sup>6</sup>–H, and C<sup>1</sup>–C<sup>6</sup> are 0.652, 0.487, 0.457, 0.307, and 0.180, respectively.